Published as: *Cell*. 2008 January 25; 132(2): 259–272.

Molecular and structural basis of cytokine receptor pleiotropy in the Interleukin-4/13 system

Sherry L. LaPorte[1], **Z. Sean Juo**[1], **Jana Vaclavikova**[1], **Leremy A. Colf**[1], **Xiulan Qi**[2], **Nicola M. Heller**[2], **Achsah D. Keegan**[2], and **K. Christopher Garcia**[1]

1*Howard Hughes Medical Institute, Departments of Molecular and Cellular Physiology, and Structural Biology, Stanford University School of Medicine, Stanford, CA 94305*

2*Center for Vascular and Inflammatory Diseases and Department of Microbiology and Immunology, University of Maryland School of Medicine, Baltimore, Maryland, 21201*

Abstract

Interleukin-4 and Interleukin-13 are cytokines critical to the development of T cell-mediated humoral immune responses, which are associated with allergy and asthma, and exert their actions through three different combinations of shared receptors. Here we present the crystal structures of the complete set of Type I (IL-4Rα/γ_c/IL-4) and Type II (IL-4Rα/IL-13Rα1/IL-4, IL-4Rα/IL-13Rα1/IL-13) ternary signaling complexes. The Type I complex reveals a structural basis for γc's ability to recognize six different γc-cytokines. The two Type II complexes utilize an unusual top-mounted Ig-like domain on IL-13Rα1 for a novel mode of cytokine engagement that contributes to a reversal in the IL-4 versus IL-13 ternary complex assembly sequences, which are mediated through substantially different recognition chemistries. We also show that the Type II receptor heterodimer signals with different potencies in response to IL-4 versus IL-13, and suggest that the extracellular cytokine-receptor interactions are modulating intracellular membrane-proximal signaling events.

INTRODUCTION

T cell-mediated immunity occurs in successive antigen-driven and cytokine-driven steps. In the first step, T cell receptors are activated by specific antigens presented by peptide-MHC complexes on the surface of antigen presenting cells. In a second step, these activated T cells are induced to clonally expand by the cytokine Interleukin-2 (IL-2), and subsequently differentiate into CD4+ Th1 or Th2 cells as a result of a specific subset of cytokines engaging and activating their respective cytokine receptors (Leonard, 1999). IL-4 is the primary cytokine implicated in the development of Th2-mediated responses (Seder and Paul, 1994), which are also associated with allergy and asthma (Barnes, 2002). The cytokines IL-4 and IL-13 are produced by Th2 cells, and recruit and activate IgE-producing B cells, and enhance IgE-mediated responses. The strong association of Th2-cytokines with allergic disease has generated interest in targeting their receptors for therapeutic intervention (Foster et al., 2002; Mueller et al., 2002).

IL-4 alpha receptor (IL-4Rα) is a unique member of the common-gamma chain (γ_c) family of receptors (Nelms et al., 1999), with the ability to signal within three different receptor complexes, known as Type I and Type II receptors (Andrews et al., 2006; Kelly-Welch et al.,

Address correspondence to: K. Christopher Garcia, kcgarcia@stanford.edu Tel# 650-498-7332.

2003; Mueller et al., 2002). On cells of hematopoietic stem cell in origin, the Type I receptor comprises IL-4Rα and the common gamma-chain (γ_c), which is also shared by the cytokines IL-2, -7, -9, -15 and -21 (Nelms et al., 1999). On cells of non-hematopoietic stem cell in origin, IL-4 can use the Type II complex, comprising IL-4Rα and IL-13Rα1 (Hilton et al., 1996; Obiri et al., 1995). This receptor complex is also a functional receptor for IL-13 (Aman et al., 1996), which shares only ~25% homology with IL-4, and this largely explains the overlap of the biological effects of IL-4 and IL-13 (Wills-Karp, 2004). Type I receptor complexes can only be formed by IL-4 and are more active in regulating Th2 development. In contrast, the Type II receptor complex formed by either IL-4 or IL-13 is not found on T cells and is more active in regulating cells that mediate airway hypersensitivity and mucus secretion (Andrews et al., 2006). In fact, IL-13 appears to have its own distinct role in allergic inflammation, acting as a key regulator of allergen-induced airway inflammation, and goblet cell metaplasia (Wills-Karp, 2004). The molecular basis for the cytokines differing functional responses is unclear. Both Type I and Type II receptor complexes signal through the Jak/STAT cascade, with IL-4Rα associating with Jak1, γ_c with Jak3, and IL-13Rα1 with Tyk2. A second mechanism of signal transduction activated by IL-4 and IL-13 leads to the insulin receptor substrate (IRS) family (Kelly-Welch et al., 2003).

IL-4 and IL-13 are prototypical four-helix bundle short chain cytokines (Moy et al., 2001; Mueller et al., 2002; Walter et al., 1992; Wlodawer et al., 1992). The IL-4/IL-13 receptors γ_c, IL-4Rα and IL-13Rα1 contain the tandem Fibronectin-III domains and the WSXWS box that form the classical elbow-shaped “Cytokine binding homology region (CHR)” which binds to the helical faces of the cytokine (Bazan, 1990), as originally defined in the human Growth Hormone (hGH) system (de Vos et al., 1992). A previous structure of a non-signaling binary complex between IL-4 and IL-4Rα indicated a similarity to the hGH-R site I paradigm (Hage et al., 1999). While the structure of a complete short-chain cytokine receptor heterodimeric signaling complex was reported for IL-2 (Wang et al., 2005), the Type I and Type II IL-4/13 receptors have several novelties that pose interesting structural questions (Mueller et al., 2002). First, in the Type II complex, the IL-13Rα1 contains an extra N-terminal Ig-like domain (D1) not found in other receptors of the γ_c subfamily, that is required for IL-13 signaling but not by IL-4 (Arima et al., 2005). It is unknown how this top-mounted Ig-like domain participates in cytokine recognition.

A second novelty pertains to cytokine receptor ‘sharing’ and the evolutionary relationships between IL-13Rα1, γ_c and IL-4Rα (Boulay et al., 2003; Leonard et al., 1994; Ozaki and Leonard, 2002). While γ_c is the primary short chain cytokine shared receptor, IL-4Rα is also shared in three signaling complexes. IL-13Rα1 bears an evolutionary relationship to γ_c (Boulay et al., 2003), but its ligand specificity is narrower and it diverged from a common ancestral family as γ_c with the acquisition of the N-terminal Ig-like domain. It will be interesting to determine if these receptors possess structural properties conducive to degenerate recognition and signaling in comparison to their highly specific alpha receptor counterparts. In addition, as only one γ_c-family complex has been solved (IL-2), the Type I complex could reveal a molecular basis for γ_c cross-reactivity.

Finally, IL-4 and IL-13 can induce distinct functional responses through the identical Type II receptor heterodimers (Kelly-Welch et al., 2003), raising the question of how ligand-specificity is conferred by shared receptors and can influence signaling. Thus, the IL-4/13 system presents an opportunity to investigate whether downstream signaling differences through common receptors have origins in the structural/biophysical properties of the extracellular receptor-cytokine complexes. In order to probe these questions, we present structural, biochemical, and signaling studies on the complete set of Type I and Type II ternary receptor complexes, IL-4Rα/γ_c/IL-4, IL-4Rα/IL-13Rα1/IL-4, IL-4Rα/IL-13Rα1/IL-13.

RESULTS

To obtain diffraction-quality crystals, we engineered glycan-minimized recombinant molecules (see Methods) that behaved similarly to wild-type glycosylated proteins, and determined the complex structures to resolutions between 2.9–3.0Å (Table S1, Figs. S1, S2). All three ternary complexes (Fig. 1) globally resemble the canonical cytokine-receptor complex architecture seen in several other cytokine receptor complexes (Stroud and Wells, 2004), albeit with substantial deviations apparent in the two Type II complexes (Figs. 1b, c, S4) (discussed below). In the three complex structures, we refer to the cytokine/IL-4Rα interfaces as site I, and the γ_c and IL-13Rα1 interfaces will be referred to as sites IIa, IIb and III (Fig. 1). The cytokines bridge the receptor heterodimers, resting in Y-shaped forks (sites I and IIa) that are buttressed underneath by extensive receptor-receptor contact forming the "stems" of the Y's (site IIb) between the D2-D2 (Type I complex) and D2-D3 domains (Type II complexes). In each complex extensive amounts of surface are buried within the cytokine-receptor and receptor-receptor interfaces (Table S2, Fig. S4) (3980Å^2 for IL-4 Type I, 4400Å^2 for IL-4 Type II, and 4030Å^2 for IL-13 Type II).

In both Type II complexes there is a novel structural feature that we term site III (Figs. 1b, c). The extra N-terminal IL-13Rα1 D1 'Ig-like' domain contacts the dorsal surfaces of both IL-4 and IL-13. The structure of the IL-13Rα1 D1 domains is an "s-type" Ig-like fold (Fig. S3) (Bork et al., 1994), where the conventional *d* strand in a top sheet of an Ig-fold now becomes a *c'* strand of the bottom sheet due to a switch in pairing (Fig. S3). This has important implications for the Type II complexes in that, by virtue of the strand swap that occurs in s-type Ig folds, the *c'* strand of IL-13Rα1 is positioned to contact the C–D loop of the cytokine through a β-sheet like interaction.

IL-13Rα1 is derived from a common ancestral subgroup as γ_c, the divergence of IL-13Rα1 is linked to the acquisition of the Ig-like domain (Boulay et al., 2003). The γ_c -cytokines IL-2 and IL-15 require unusual 'sushi' domain alpha receptors for formation of the "high affinity" IL-2/IL-15-Rαβγ_c complexes (Fig. 2a) (Waldmann, 2006). The IL-2Rα and IL-15Rα bind to the dorsal surfaces of the cytokines (Fig. 2a, c) (Chirifu et al., 2007; Rickert et al., 2005), at locations overlapping with the IL-13Rα1 D1 binding sites on IL-4 and IL-13 (Fig. 2b, c). From the ancestral relationship of IL-13Rα1 and γ_c, it is tempting to speculate that the top-mounted D1 domain of IL-13Rα1 has structural and functional analogies to IL-2/IL-15Rα. Possibly the divergence of three-domain IL-13Rα1 from the two-domain γ_c subgroup is the result of a gene fusion event between a separate Ig-like domain receptor (analogous to IL-2/IL-15Rα) and the IL-13Rα1 D2D3 module (Fig. 2b), consolidating both receptors on a single polypeptide chain.

Diverse ternary complex assembly energetics

The three complexes form by the sequential, and cooperative assembly, of composite cytokine-receptor binding surfaces that exhibit striking differences in the extent and distribution of polar and apolar surfaces (Fig. S4, and Tables S2, contact Tables S4–S7). In order to determine whether this structural diversity is reflected in diverse binding chemistries, we investigated the complex assembly thermodynamics using Isothermal Titration Calorimetry (ITC) with soluble receptor extracellular domains (ECDs) (Fig. 3, Table S3). Consistent with previous studies (Andrews et al., 2002; Obiri et al., 1995; Russell et al., 1993), we find in the Type I complex, IL-4 first binds to IL-4Rα, followed by recruitment of γ_c to form a ternary complex (Fig. 3a). For the Type II IL-4 complex, IL-4 again first binds to IL-4Rα followed by recruitment of IL-13Rα1 (Fig. 3b). In contrast, for the Type II IL-13 complex, IL-13 first binds IL-13Rα1 with an affinity of K_d = 30nM (similar to previous BIAcore studies (K_d = 34nM, (Andrews et al., 2002)) and this binary complex then recruits IL-4Rα (Fig. 3c). Strikingly, in the Type I and II IL-4 complexes, the same IL-4/IL-4Rα binary complex engages γ_c and IL-13Rα1 through opposite thermodynamic profiles (Figs. 3a,b – far right, Table S3), in which the Type I complex

shows a strongly favored enthalpy ΔH= −11.7 kcal/M, and a disfavored entropy ΔS = −10.5cal/molK^{-1}, compared to the Type II complex showing a weakly favored enthalpy ΔH= −4.8 kcal/M and strongly favorable entropy ΔS = 13.0cal/molK^{-1}. Further, even in a case where several key interfacial residues persist, such as the site I interface of IL-4Rα with IL-4 (ΔH= −11.2kcal/mol, ΔS= +3.5cal/molK^{-1}) versus IL-13 (ΔH= −5.8kcal/mol, ΔS = +16.0cal/molK^{-1}), distinct thermodynamic binding signatures are observed (Figs. 3a, b, c, Table S3). Although in our structures it is difficult to visualize trapped water molecules potentially impacting the entropy of the interactions, our results show that these shared receptors utilize diverse binding thermodynamics tailored to each ligand, in contrast to the basis of cross-reactivity in the gp130 system, which has converged on a desolvation-driven mechanism for all of its ligands (Boulanger et al., 2003).

With respect to formation of the ternary signaling complexes, the IL-13 Type II appears to be the most stable by virtue of a higher affinity of the IL-13/IL-13Rα1 binary complex for IL-4Rα (K_d = 20nM) (Fig. 3c – far right, Table S3). The IL-4 Type I and Type II complexes both have very low affinity interactions with γ_c (K_d = 559nM), similar to BIAcore measurements (Andrews et al., 2006;Zhang, 2002) and IL-13Rα1 (K_d = 487nM), respectively, resulting in lower overall complex stabilities (Fig. 3a,b – far right). Thus, the recruitment of the second 'trigger' receptors appears energetically limiting for the IL-4 complexes and could play a role in the differential signaling properties of the IL-4 versus IL-13 complexes (discussed later).

The site I interactions of IL-4Rα with IL-4 versus IL-13

The interactions seen in the Type I and Type II IL-4/IL-4Rα interfaces are similar to the previously reported IL-4/IL-4Rα binary complex (Hage et al., 1999) (Fig. 4a), except that in the ternary complexes the IL-4Rα FN-III domains are rotated several degrees 'counterclockwise' around the IL-4 helical bundle, likely due to the interactions formed between the bases of the receptors (i.e. the stem of the Y). The principal feature of the large IL-4/IL-4Rα interface (Figs. 4a, S4) remains a charge complementarity between patches centered on "hotspot" residues Glu9 and Arg88 on the IL-4 A and C helices (Fig. 4a) (Zhang et al., 2002), respectively, which form polar contacts with Tyr13, Tyr183, Ser70, and Asp72 on IL-4Rα.

The site I interface of IL-13 with IL-4Rα (Fig. 4b) is presented on a more compact IL-13 helical scaffold (see Figs. 1b,c top view) (two helical turns shorter in both A and C helices than IL-4). Although the binding surface and amino acids used on IL-4Rα to bind IL-13 are nearly identical to that used to contact IL-4 (Fig. 4a), their four-helix bundles superimpose poorly when the complexes are aligned on IL-4Rα (Fig. 4c). Yet, IL-13 exactly recapitulates two critical charged residues by presenting Glu12 and Arg65 to IL-4Rα in the same positions to form similar receptor contacts as seen for IL-4 residues Glu9 and Arg88 (Figs. 4b–d), which have been shown by mutagenesis to be energetically important (Kraich et al., 2006). However, the composition of remaining IL-13 contact residues with IL-4Rα is different (Fig. 4c, d), in accord with the distinct binding thermodynamics the two cytokines use to bind IL-4Rα(Figs. 3b, c,Table S3). In the IL-13/IL-4Rα site I, the interface lacks interactions ringing the charged hotspots observed in the IL-4/IL-4Rα interface, such as the loss of IL-4 residue Trp91 on the C helix (Fig. 4c). The number of polar bonds per 100Å^2 of surface buried in the IL-13/IL-4Rα interface is 1.0, denoting a substantial loss in specificity relative to the extraordinarily specific IL-4/IL-4Rα complex (2 polar bonds per 100Å^2). Given that IL-4 binds to IL-4Rα with sub-nanomolar affinity, and IL-13 has no measurable affinity for IL-4Rα alone, the energetic value of the two 'mimicked' charged contacts on IL-13 (Kraich et al., 2006) is apparently manifested within the context of the 'composite' interface formed together with the

receptor-receptor contacts (site IIb). In this fashion, the IL-4Rα/IL-13 site I works in concert with site IIb to engage IL-4Rα through tandem, multi-point attachment of two weak interfaces.

The site IIa and site III interactions

The formation of the ternary signaling complex is completed by the recruitment of a second receptor, either γ_c or IL-13Rα1 through structurally separated binding contacts designated sites IIa (fork of the Y) (Table S5), IIb (stem of the Y) (Table S6) and, in the cases of the Type II complexes, site III (Table S5).

The three site IIa interfaces are uniformly characterized by the convex elbow of the receptors occupying a canyon on the A and D helices of the cytokines (Figs. 5a–c), exhibiting excellent knob-in-holes shape complementarity (Table S2)(Sc = 0.82, 0.73 and 0.65 for the IL-4 Type I, and IL-4 and IL-13 Type II complexes, respectively). Several hydrogen bonds flank the sides of the apolar canyons in each complex, and likely stabilize the respective docking orientations. Consistent with their ancestral relationship, IL-13Rα1 and γ_c present binding sites with convergent structural features (Figs. 5a, b). The site IIa contacts in each of the receptor complexes are primarily formed by the FG2 loop of the membrane proximal FN-III domains of γ_c and IL-13Rα1 (D2 and D3, respectively), but γ_c also uses the EF1 loop in its D1. The receptor binding surfaces present a somewhat chemically inert main chain surface that inserts into a cleft in the bases of cytokines. Both γ_c and IL-13Rα1 insert an unusual surface-exposed disulfide bond linking the FG2 and BC2 loops, together with a neighboring side chain (Leu208 for γ_c, Leu319 for IL-13Rα1) into the cavity on the cytokine surface (Figs. 5a–c). One substantial deviation between γ_c and IL-13Rα1 is that γ_c also forms extensive van der Waals contacts with IL-4 through Tyr103 on the EF1 loop of the D1 domain, resulting in a two-point site IIa attachment to IL-4 (Fig. 5a). This EF-loop interaction is missing in both Type II complexes (Figs. 5b, c), consistent with mutational data on the IL-13Rα1 EF loop showing minor effects on binding (Arima et al., 2005).

A stripe of amino acids on the IL-4 and IL-13 A and D helices demarcates the hydrophobic canyon lined by the alkyl moieties of both polar and non-polar amino acids (Figs. 5d, e). These side chains part to both sides to form clefts into which the narrow receptors insert to contact the main chains of the cytokine helices, facilitating degenerate recognition. (Figs. 5b,c). The canyon on IL-4 engages non-identical amino acids on γ_c versus IL-13Rα1 in structurally similar fashions (Figs. 3a, b). For example, IL-4 residues Gln8, Ile11, Asn15 interact with γ_c Pro207 and Leu208, which appear to serve as structural equivalents Lys318 and Leu319 of IL-13Rα1 (Figs. 5a,b). Although the binding canyons on IL-4 and IL-13 utilize different amino acids to engage their receptors, they retain similar surface and shape properties, suggesting a manner of convergent structural evolution to enable cross-reactivity.

The most unique structural feature in the Type II complexes is site III (Figs. 5f, g). The principal structural characteristic of site III is an anti-parallel beta sheet between the *c'* strand of IL-13Rα1 and the C–D strand of IL-4 and IL-13. Similar sheet-like contacts form between IL-4 strand residues Asn105 to Thr108, or IL-13 residues Thr88 to Glu91, to the *c'* strand residues of IL-13Rα1 Lys76 to Ile78. However, there is an additional source of contact in the IL-13 site III that may explain the requirement of the IL-13Rα1 D1 for signaling in the IL-13 Type II complex, in contrast to IL-4 (Arima et al., 2005). We also found in mutational studies that after deletion of IL-13Rα1 D1, the D2D3 CHR module alone does not detectably bind to IL-13, whereas IL-13Rα1 D2D3 does form a ternary complex with IL-4/IL-4Rα(Fig. S5). In the IL-13 complex site III (Fig. 5g), a prominent saucer-shaped, hydrophobic patch on the IL-13 surface is formed by the alkyl sides chain of Met 33, Asp87, Lys89, and Trp35, creating a surface apposing an hydrophobic patch on the tip of IL-13Rα1 D1 composed of Trp65 and Ile78 on the c' strand (Table S2, Fig. S4). By contrast, the analogous region of IL-4 lacking the complementary hydrophobic patch (Figs. 5f, S4), is apparently relatively devoid of energetic

value. However, as for the site IIa energetics, the energetic basis of the respective IL-13Rα1 D1-dependencies for IL-4 and IL-13, is not explained by the structure of site III alone, but likely highly energetically coupled to sites IIa (for IL-13) and sites IIa/IIb (for IL-4).

Receptor-receptor interactions (site IIb) within the ternary complexes

In all three complexes, extensive contacts (~1200–1300Å^2 BSA) are formed between the membrane-proximal domains of the receptors (Fig. S4 & Table S2). Although the sequences of γ_c and IL-13Rα1 are highly divergent (26% identity), the site IIb interactions appear to utilize a limited degree of molecular mimicry to engage the shared IL-4Rα in that several pair-wise amino acid contacts are replicated. For example, both γ_c and IL-13Rα1 use structurally equivalent Phe186 and Phe297, and Pro189 and Pro300, respectively, to interact with a hydrophobic stretch of IL-4Rα *d* strand residues Tyr150 through Tyr159 (Table S6). The receptor-receptor interfaces have very poor shape complementarity values of 0.49, 0.52 and 0.57 for the three complexes. By comparison, the excellent shape complementarity of the site IIa interfaces would appear to suggest that the cytokine-receptor contact is the primary driving force for site II formation. Collectively, the three weak interactions alone (sites IIa, IIb and III), cooperatively form a tripartite binding site where productive affinity is achieved through multi-point attachment.

How does γ_c cross-react with six different cytokines?

γ_c is a signaling receptor for at least six different short-chain cytokines, including IL-2, -4, -7, -9, -15 and -21 (Ozaki and Leonard, 2002). Previously we determined the structure of the quaternary complex of IL-2 with IL-2Rα, IL-2Rβ, and γ_c (Wang et al., 2005). With a second γ_c ternary complex, we analyzed how γ_c can engage six cytokines with less than 15% sequence identity (Fig. 6). The IL-2 and IL-4 interfaces with γ_c are strikingly similar, both burying ~1000 Å^2, having similar ratios of polar/apolar surface, and low specificity indices (0.7–1.0 polar bonds/100Å^2). The γ_c binding sites on IL-2 and IL-4 exhibit apolar 'canyons' that receive the protruding elbow of γ_c through near-ideal shape complementarity (Fig. 6b) (Sc for IL-4 site IIa is 0.82, for IL-2 is 0.82). γ_c residues Tyr103 and the disulfide Cys160-Cys209 engage the IL-4 canyon in a coupled manner as seen in the IL-2-γ_c interface (Fig. 6b). Cytokine contact residues on γ_c loops BC2 and FG2 maintain similar conformations in both IL-2 and IL-4 complexes, suggesting that cross-reactivity is not occurring through structural plasticity of the receptor, but rather a rigid γ_c surface encounters extraordinarily complementary shape features on γ_c-cytokines, which are further enhanced by specific hydrogen bonds peripheral to the canyon.

When IL-2 and IL-4 carbon-α (abbrev. Cα) positions are compared in the complexes (Fig. 6c), five residues each on helices A and D overlap with a very close r.m.s. deviation. of 0.2 Å and 0.3 Å, respectively, as compared with the overall IL-2/IL-4 r.m.s.d. of 1.7 Å. The structurally equivalent side chains of IL-2 residues Glu15, Leu19, Gln126, Ser130 and IL-4 residues Gln8, Lys12, Arg121, Ser125 collectively line the complementary canyon, making analogous interactions with γ_c (Fig. 6c). Several key hydrophobic residues within the helical core, which dictate the resultant positions of "external" interacting side chains on the helices, are conserved (Fig. 6d). We propose these cytokine residue positions constitute a γ_c "recognition motif" that likely demarcates residues serving similar structural roles in other γ_c-cytokine complexes.

Signaling by the Type I and Type II receptor complexes on cells

Given the shared use of receptors in the IL-4/13 system, we asked what the relative potencies of receptor activation were for IL-4 versus IL-13 through the Type I and II receptors on cell lines (Fig. 7). Since engagement of the Type I and Type II receptor complexes leads to the activation of STAT6 (Kelly-Welch et al., 2003), we compared the IL-4-and IL-13-induced phosphorylation of STAT6 as a measure of receptor complex activation (Fig. 7). In addition,

we analyzed the phosphorylation of STAT3 (Fig. S6). We analyzed signaling by the Type I IL-4 receptor in the human B-cell line Ramos, which express γ_c and IL-4Rα. We analyzed signaling by the Type II receptors in the human epithelial carcinoma cell line A549, which express IL-4Rα and IL-13Rα1, but do not express the γ_c or the decoy receptor IL-13Rα2 (Fig. 7a). Treatment of A549 cells with either IL-4 or IL-13 for 30 minutes stimulated the potent tyrosine phosphorylation of STAT6 and the relatively weak phosphorylation of STAT3 (Figs. 7b, S6). IL-4 was able to stimulate phosphorylation at significantly lower doses (five to ten-fold) than IL-13. Treatment of Ramos cells with IL-4 stimulated the tyrosine phosphorylation of STAT6 with a dose-response similar to that observed on A549. We also examined the kinetics of STAT6 and STAT3 phosphorylation at several cytokine concentrations (Figs. 7c, S6, S7). At all concentrations tested (1, 5, 50 ng/ml), IL-4 rapidly induced the tyrosine phosphorylation of STAT6 in A549 reaching plateau levels between 10–15 minutes of stimulation. However, the response to IL-13 was substantially slower. Treatment of A549 cells with 1 ng/ml, 5 ng/ml or 50 ng/ml stimulated the tyrosine phosphorylation of STAT6 to plateau levels at >60, 30, and 15 minutes respectively. The relative delay in STAT6 phosphorylation induced by IL-13 via the Type II receptor complex was most apparent at lower concentrations of cytokine (1 ng/ml). (Figs. S6, S7). The stimulation of STAT3 phosphorylation by either IL-4 or IL-13 was quite weak in these cells, however, the pattern of responsiveness was similar to what we observed for STAT6 (Fig. S6). Treatment of Ramos cells with IL-4 stimulated the tyrosine phosphorylation of STAT6 with kinetics similar to that observed on A549; IL-4 achieved maximal phosphorylation between 10–15 minutes of stimulation (Figs. 7c, S7). We did not observe the induction of STAT3 phosphorylation by IL-4 in these cells (Fig. S6). The implications of these signaling data in the context of the structural and thermodynamic data are discussed further below.

DISCUSSION

The results presented here on the IL-4/13 system bear on several coupled issues in ligand-receptor interactions, namely: 1) the structural basis of degeneracy versus specificity of shared receptors, 2) the assembly energetics and sequences of hetero-dimeric receptor complexes, and 3) whether differences in these *extracellular* parameters could qualitatively influence the coupling of ligand engagement to *intracellular* receptor activation. Surprisingly, we found that that the identical Type II receptor heterodimer, coupled to the same intracellular signaling molecules, responds to different ligands, IL-4 versus IL-13, with different signaling potencies and kinetics (Figs. 7b, c, S6, S7). One can consider the initial cytokine-receptor interaction as the ‘driver,’ and the second receptor recruited for ternary complex signaling as the ‘trigger’, akin to terminology previously proposed for the assembly of γ_c heterodimeric complexes (Lai et al., 1996). The IL-4/13 system has the unique property that IL-4 and IL-13 have swapped their trigger and driver. The evolutionary expansion of receptor usage by switching 'driver' and 'trigger' modules has also occurred in other receptors in the family, such as IL-7Rα/γ_c (Noguchi et al., 1993) and IL-7Rα/TSLP-R (Pandey et al., 2000). In the IL-4/13 system this switch is mainly due to the acquisition of the energetically critical site III in IL-13, and the ‘hobbling’ of its site I. From previous studies we know that the equilibrium binding affinities of IL-4 and IL-13 for their heterodimeric receptor complexes on cell surfaces are similar (K_d ranging from 30–400 pM) (Aman et al., 1996; Andrews et al., 2002; Hilton et al., 1996; Park et al., 1987), so the explanation for the potency differences is not simply receptor occupancy. The fact that IL-4 binds to the IL-4Rα with very high affinity (K_d~ sub-nanonomolar) (Andrews et al., 2006; Park et al., 1987), and the presence of γ_c or IL-13Rα1 provides little additional affinity (Murata et al., 1998; Russell et al., 1993; Zhang, 2002) suggests that driver association is dictating IL-4 Type II signaling potency. Yet, we find that the high affinity driver complex (IL-4/IL-4Rα) recruits the IL-13Rα1 ‘trigger’ receptor with very low affinity (K_d ~ 487nM), which would be energetically rate-limiting for signaling. In contrast, IL-13 initially binds to its driver receptor (IL-13Rα1) on the surface of cells with a relatively slow on-rate, but still

with a moderately strong binding constant (K_d ~30nM) (Aman et al., 1996; Hilton et al., 1996). However, the presence of its trigger IL-4Rα increases the cell surface affinity for IL-13 from K_d ~ 10 nM to 30 pM (Miloux et al., 1997). Thus, the recruitment of the trigger receptor (IL-4Rα) by the IL-13/IL-13Rα1 driver complex is more energetically favorable (K_d ~20nM) than is the converse trigger receptor (IL-13Rα1) recruitment by the IL-4/IL-4Rα driver complex (K_d ~487nM). Yet, paradoxically, we find that IL-4 is more potent at stimulating the tyrosine phosphorylation of STAT6 in several cell lines.

From the aforementioned energetic results we would predict that if the trigger receptor becomes limiting, the sensitivity and kinetics of STAT6 phosphorylation may change. Based on estimates in cell lines, the numbers of IL-4Rα chains (50–5000 molecules/cell) appears to be limiting as compared to the numbers of IL-13Rα1 chains (5000–150,000 molecules/cell) (Park et al., 1987, Obiri et al., 1995). In the two cell lines we analyzed herein, expression of the IL-4 trigger receptor (γc or IL-13Rα1) was greater than IL-4Rα (Fig. 7a). However, in cells where IL-13Rα1 is limiting, IL-13 can become more potent than IL-4 (William Paul, Ilkka S. Juntilla, Kiyoshi Mizukami, Harold Dickenstein, Martin Meier-Schellersheim, Raymond P. Donnely (NIH), personal communication). Thus, it appears that when the IL-4 trigger receptor (IL-13Rα1) is abundant, the high affinity IL-4/IL-4Rα driver complex determines the ultimate signaling potency. By comparison, the affinity of IL-13 for its driver IL-13Rα1 (K_d ~30nM), results in efficient formation of the IL-13/IL-13Rα1 driver complex even when IL-13Rα1 is limiting, and the substantially higher affinity of the IL-13/IL-13Rα1 driver complex for its trigger receptor (IL-4Rα) (K_d ~ 20nM) could result in more potent IL-13 signaling versus IL-4. Thus, the potency of signal transduction can be influenced by a variety of physical-chemical properties that are communicated through the cytokine receptor ECD interactions, including the concentration of cytokine and expression levels of receptor, the order of assembly of the signaling complexes, and the affinities of ‘trigger’ and ‘driver’ receptor recruitment. *In vivo*, the potential for higher order assemblies of receptors on the cell surface, soluble shed receptors in the extracellular millieu, and the expression of the non-signaling IL-13Rα2 serving as a decoy, could play unknown roles in IL-4/13 signaling regulation.

Although highly speculative, another possible contributing factor to the enhanced potency of IL-4 may lie in the relative *orientations* of the receptor heterodimers in the two complexes. It has been shown for gp130 and the Erythropoietin receptor (EPO-R) that perturbations in the rotational “pitch” of the membrane-proximal intracellular regions, which are proximal to the Jak binding sites, can modulate signaling potency (Constantinescu et al., 2001; Greiser et al., 2002). Additionally, one study examined structures of complexes of EPO-R ectodomains with synthetic peptide agonist and antagonist mimics of EPO (Livnah et al., 1998), and found the antagonist complex was rotated approximately 14 degrees away from the two-fold axis compared to the agonist complex (Fig. S8b). We find that, when the IL-4 and IL-13 Type II complexes are superimposed on either IL-4Rα or IL-13Rα1, the relative orientation of the membrane-distal domains of the ‘partner’ receptor differs by ~7–8 degrees (Fig. S8a). The origin of this difference appears to lie mainly in the IL-4 versus IL-13 site I interfaces, which have diverged more in their relative cytokine/receptor positioning than the membrane-proximal regions. This perturbation in orientation could (Fig. S8), in principle, exert a modulatory role on signaling in a fashion analogous to the EPO peptide mimetics, although this remains speculative.

Collectively, our structural, biochemical and signaling results invite revision of the concept that extracellular ligand engagement of cytokine receptors does not relay ‘instructive’ information intracellularly. Experiments in which the ECD of EPO-R was replaced with the Prolactin ECD, resulting in red blood cell formation, concluded that structurally indiscriminate dimerization was adequate to initiate cytokine receptor signaling (i.e ‘permissive signaling’) (Socolovsky et al., 1998). While we concur that downstream signaling specificity is manifested

intracellularly, our results appear to suggest that the potency of receptor signaling can be influenced by the biophysical and structural properties of the extracellular receptor-ligand interactions, which may, in this case, be utilized as a means for different ligands to induce divergent signaling responses through shared receptors in different cellular contexts.

METHODS

Ternary complex protein expression and purification

Human IL-4, IL-13, and the ectodomains of γ_c, IL-4Rα, and IL-13Rα1 cDNA were sub-cloned into pAcGP67-A with C-terminal hexahistidine tags (BD Biosciences, San Diego, CA), and secreted from High-Five™ insect cells in Insect-Xpress™ medium (Lonza, Walkersville, MD). In order to reduce protein heterogeneity due to Asn-linked glycosylation, we expressed the molecules in various glycan-minimized forms. IL-4 was expressed in the presence of tunicamycin (2.5 mg/L) (Calbiochem, San Diego, CA) to suppress Asn-linked glycosylation. For IL-4Rα we mutated Asn➔Gln in four, out of a possible six, N-linked glycosylation sites (N28Q, N73Q, N109Q, N151Q). IL-13 and IL-13Rα1 were co-expressed in the presence of tunicamycin (0.65 mg/L). For the Type I complex, each component was separately purified by gel filtration FPLC Superdex 200 (GE Heathcare, Piscataway, NJ) after which a 1:1:1 molar ratio of IL-4, IL4Rα and γ_c was mixed, digested with carboxypeptidase A (EMD Biosciences, San Diego, CA) to remove C-terminal His-tags, and then re-purified by gel filtration. The IL-4 Type II complex was produced in a similar fashion for crystallization trials, using IL-13Rα1 expressed in the presence of tunicamycin. For the IL-13 Type II complex, IL-13 and IL-13Rα1 co-expressed in the presence of tunicamycin was digested with carboxypeptidase A and purified as a binary complex by gel filtration. The IL-4Rα tetra-glycan mutant was separately expressed and purified, and added to the binary complex in a 1:1:1 ratio, and purified by MonoQ FPLC. Ternary complex molecular masses were confirmed by MALS analysis.

Isothermal Titration Calorimetry (ITC)

Calorimetric titrations were carried out on a VP-ITC calorimeter (MicroCal, Northhampton, MA) at 27 °C. Gel filtration purified samples were dialyzed into sterile filtered 10 mM Hepes, pH 7.2, 150mM NaCl. Data were processed with OriginLab software. Protein concentrations were determined using the BCA method. The *n*, or stoichiometry values determined by ITC vary by ~25% (e.g. *n* values between 0.7 and 1.3 for an *n* value of 1.0) and are consistent with gel filtration molecular weight estimation. In the titrations of binary complexes, the titrand was used in the cell at a concentration of 5 μM (IL-13Rα) or 8 μM (IL-4Rα), and the titrant in the syringe at a concentration 81 μM (IL-13) or 65 μM (IL-4). In the titration of the ternary complexes two approaches were used in order to compare similar complexes. Preformed and purified 1:1 IL-4/IL-4Rα binary complex (55–57 μM) was titrated into either γ_c (8 μM) or IL-13Rα1 (3 μM). Conversely, preformed and purified 1:1 IL-13/IL-13Rα1 binary complex (3 μM) was the titrand in the cell while IL-4Rα (22 μM) was the titrant in the syringe.

Ternary complex crystallization and X-ray Data Collection

The IL-4Rα/γ_c/IL-4 ternary (8–12 mg/ml) was screened for crystallization using sparse matrix crystallization reagent Wizard III (deCODE Biostructures, Bainbridge Island, WA). Crystals grew in 8–12% PEG 8000, 0.1 M HEPES pH 7.5, and 8% ethylene glycol. Data collection was performed at the beamline 11-1, Stanford Synchrotron Radiation Laboratory (SSRL). The crystals diffracted to 2.95 Å resolution in space group $P2_12_12_1$, with unit cell dimensions of a = 52.58 Å, b = 86.65 Å, c = 175.67 Å. The data set was indexed, integrated, and scaled with HKL2000 (Otwinowski and Minor, 1997).

The IL-4Rα/IL-13Rα1/IL-4 ternary complex grew in conditions containing 5–10% PEG 8000, 0.1 M cacodylate pH 6.5, 0.16 M calcium acetate, and 20% glycerol. Data collection was

performed at beamline 8.2.2, Advanced Light Source (ALS), University of California, Berkeley. The crystals diffracted to 3.0 Å resolution in the space group $P2_1$, with unit cell dimensions of a = 61.64 Å, b = 62.84 Å, c = 115.13 Å, and β = 96.31°. The data set was indexed, integrated, and scaled with HKL2000 (Otwinowski and Minor, 1997).

For the IL-4Rα/IL-13Rα1/IL-13 ternary complex two crystal forms were obtained, using either the fully glycosylated IL-4Rα(form I), or the quadruple glycosylation knock-out version as described above (form II). The form I crystals grew in 10–15 % PEG 8000, 8% ethylene glycol, 0.1 M ammonium citrate pH 6.0, and were cryopreserved in 23% ethylene glycol. Data collection was performed at ALS beamline 8.2.1. The crystals diffracted to 3.5 Å resolution with anisotropic diffraction extending to 3.2 Å, and belong to space group $P2_12_12_1$, with unit cell dimensions of a = 91.98 Å, b = 125.10 Å, c = 148.27 Å, with two copies of the complex per asymmetric unit. Data was indexed, integrated, and scaled with HKL2000 (Otwinowski and Minor, 1997).

The higher resolution, glycan-minimized form II crystals were obtained in 12% PEG 6000, 0.2 M ammonium citrate, and 20% glycerol, and cryo-protected with 15% ethylene glycol. These crystals diffracted at SSRL BL 11-1 to 3.0 Å with anisotropic diffraction extending to 2.8 Å. They belong to the space group C2, with unit cell dimensions of a = 211.51 Å, b = 58.17 Å, c = 64.24 Å, with one copy of the complex per asymmetric unit. The data set was indexed, integrated and scaled with Mosflm and SCALA as implemented in CCP4 (CCP4, 1994).

Structure Determination and Refinement

The IL-4Rα/γ_c/IL-4 ternary complex structure was determined by molecular replacement (MR) with the program Phaser (McCoy, 2007) from the CCP4 program suite (CCP4, 1994), using the binary complex of IL-4/IL-4Rα (pdb access code 1IAR) and the γ_c chain from the IL-2 quaternary complex (pdb access code 2B5I) as search models. Rigid-body refinement on the molecular replacement solution, followed by simulated annealing and individual B-factor refinement were performed using CNS. After model rebuilding with COOT based on composite omit maps, and further refinement with CNS and Refmac5 (Brunger et al., 1998; Emsley and Cowtan, 2004; Murshudov et al., 1997), the final R_{cryst} and R_{free} were 22.6% and 29.7%, respectively. For this as well as the two structures described below, Procheck (Laskowksi, 1993) indicates that Ramachandran statistics and the geometry of the protein models are compatible with structures at similar resolutions (Table 1).

For the IL-4Rα/IL-13Rα1/IL-13 ternary complex, MR solutions were obtained using the diffraction data of form I crystals (with fully glycosylated IL-4R), with IL-4R as the search model (pdb access code 1IAR). These solutions enabled the establishment of a non-crystallographic symmetry (NCS) operator relating molecules. Phaser also identified one MR solution for IL-13, by searching with the averaged IL-13 NMR model (pdb access code 1IJZ), and the second copy of IL-13 was properly placed into the crystal lattice using the NCS operator. Rigid-body refinement was performed on the MR solutions of the IL-4Rα/IL-13 binary complex. Subsequently, the D2D3 portion of IL-13Rα1 was obtained by Molrep (Vagin and Teplyakov, 2000) using a “culled” receptor model based on the D2D3 domains of gp130 (pdb access code 1BQU). The second copy of the IL-13Rα1 D2D3 domains was then placed using the NCS operator, and the partial model was rigid-body refined using CNS. The diffraction data of higher resolution from the form II crystals of the IL-4Rα/IL-13Rα1/IL-13 ternary complex was used for model rebuilding and refinement. After molecular replacement with Phaser to place the partially refined ternary complex model into the current crystal lattice, several rounds of multi-crystal averaging improved the density maps, allowing the rebuilding of the D2D3 domains of IL-13Rα1. The remaining D1 domain of 13Rα1 was placed into the complex with Phaser, using a fibronectin type III domain structure (pdb access code 1FNA) as search model. Following rigid body refinement, reiterations of model rebuilding with COOT

and structure refinement using CNS and Refmac5, the final R_{cryst} and R_{free} for this ternary complex were 25.6% and 31.2%, respectively (Table 1).

For the remaining IL-4Rα/IL-13Rα1/IL-4 ternary complex, the MR search was performed with Phaser, using models from the other two complexes. Following rigid body refinement, model rebuilding using COOT and structure refinement with CNS and Refmac5, the R_{cryst} and R_{free} were 23.8% and 30.4%, respectively (Table 1).

Analysis of Receptor Expression and STAT phosphorylation

Expression of receptor subunits was analyzed by FACS. PE-conjugated antibodies to human IL-4Rα, γ_C, and IL-13Rα1 were from BD Pharmingen (San Diego, CA); PE-conjugated anti-IL-13Rα2 was from Cell Sciences (Canton, MA). The signaling experiments were performed as described previously (Zamorano et al., 1996). Briefly, A549 or Ramos cells were washed 3 times and treated with various concentrations of IL-4 or IL-13 (R & D Systems Minneapolis, MN) for various times. Cells were harvested and lysed. Equal amounts of protein (~1 mg) were immunoprecipitated with rabbit anti-STAT6 (S-20, Santa Cruz Biotechnology, CA). The samples were separated on 7.5% SDS-PAGE, and transfered to polyvinylidene difluoride (PVDF) membrane. The membranes were probed with an anti-phosphotyrosine antibody, RC20-H (Transduction Labs, Lexington, KY). The bound antibody was detected using enhanced chemiluminescence. Where indicated the blots were stripped and probed with anti-STAT6. In some cases, total cell lysate (30 μg/lane) was analyzed using anti-phospho-specific STAT6 (Y641) or STAT3 (Y705) antibodies (Cell Signaling Technology, Danvers, MA). The films were scanned and analyzed using NIH Image. The density of signal from the phospho-STAT6 was normalized to the density of total STAT6, and expressed as phosphorylated STAT6/total STAT6 ratios. The calculated percent maximum from 3 independent experiments was averaged and graphed +/− SEM. The student's T-test was used to determine the significance of differences between groups.

Supplementary Material

Refer to Web version on PubMed Central for supplementary material.

ACKNOWLEDGMENTS

The authors gratefully acknowledge Jean-Louis Boulay, William Paul, Ilkka S. Juntilla, Kiyoshi Mizukami, Harold Dickenstein, Martin Meier-Schellersheim, Raymond P. Donnely (NIH) for discussion and sharing of unpublished data. This work was supported by the Sandler Program for Asthma Research (KCG, SL), the American Cancer Society (SL), National Science Foundation (LC), Howard Hughes Medical Institute (KCG) and NIH (AI51321) (KCG), AI38985 (ADK) and T32 HL007698 (NMH).

LITERATURE CITED

Aman MJ, Tayebi N, Obiri NI, Puri RK, Modi WS, Leonard WJ. cDNA cloning and characterization of the human interleukin 13 receptor alpha chain. J Biol Chem 1996;271:29265–29270. [PubMed: 8910586]

Andrews AL, Holloway JW, Holgate ST, Davies DE. IL-4 receptor alpha is an important modulator of IL-4 and IL-13 receptor binding: implications for the development of therapeutic targets. J Immunol 2006;176:7456–7461. [PubMed: 16751391]

Andrews AL, Holloway JW, Puddicombe SM, Holgate ST, Davies DE. Kinetic analysis of the interleukin-13 receptor complex. J Biol Chem 2002;277:46073–46078. [PubMed: 12354755]

Arima K, Sato K, Tanaka G, Kanaji S, Terada T, Honjo E, Kuroki R, Matsuo Y, Izuhara K. Characterization of the interaction between interleukin-13 and interleukin-13 receptors. J Biol Chem 2005;280:24915–24922. [PubMed: 15870068]

Barnes PJ. Cytokine modulators as novel therapies for asthma. Annu Rev Pharmacol Toxicol 2002;42:81–98. [PubMed: 11807165]

Bazan JF. Structural design and molecular evolution of a cytokine receptor superfamily. Proc Natl Acad Sci U S A 1990;87:6934–6938. [PubMed: 2169613]

Bork P, Holm L, Sander C. The immunoglobulin fold. Structural classification, sequence patterns and common core. J Mol Biol 1994;242:309–320. [PubMed: 7932691]

Boulanger MJ, Bankovich AJ, Kortemme T, Baker D, Garcia KC. Convergent mechanisms for recognition of divergent cytokines by the shared signaling receptor gp130. Mol Cell 2003;12:577–589. [PubMed: 14527405]

Boulay JL, O'Shea JJ, Paul WE. Molecular phylogeny within type I cytokines and their cognate receptors. Immunity 2003;19:159–163. [PubMed: 12932349]

Brunger AT, Adams PD, Clore GM, DeLano WL, Gros P, Grosse-Kunstleve RW, Jiang JS, Kuszewski J, Nilges M, Pannu NS, et al. Crystallography & NMR system: A new software suite for macromolecular structure determination. Acta Crystallogr D Biol Crystallogr 1998;54(Pt 5):905–921. [PubMed: 9757107]

CCP4. The CCP4 suite: programs for protein crystallography. Acta Crystallogr D Biol Crystallogr 1994;50:760–763. [PubMed: 15299374]

Chirifu M, Hayashi C, Nakamura T, Toma S, Shuto T, Kai H, Yamagata Y, Davis SJ, Ikemizu S. Crystal structure of the IL-15-IL-15Ralpha complex, a cytokine-receptor unit presented in trans. Nat Immunol 2007;8:1001–1007. [PubMed: 17643103]

Constantinescu SN, Huang LJ, Nam H, Lodish HF. The erythropoietin receptor cytosolic juxtamembrane domain contains an essential, precisely oriented, hydrophobic motif. Mol Cell 2001;7:377–385. [PubMed: 11239466]

de Vos AM, Ultsch M, Kossiakoff AA. Human growth hormone and extracellular domain of its receptor: crystal structure of the complex. Science 1992;255:306–312. [PubMed: 1549776]

DeLano, WL. The PyMOL Molecular Graphics System. Palo Alto, CA, USA: DeLano Scientific; 2002.

Emsley P, Cowtan K. Coot: model-building tools for molecular graphics. Acta Crystallogr D Biol Crystallogr 2004;60:2126–2132. [PubMed: 15572765]

Foster PS, Martinez-Moczygemba M, Huston DP, Corry DB. Interleukins-4, - 5, and -13: emerging therapeutic targets in allergic disease. Pharmacol Ther 2002;94:253–264. [PubMed: 12113801]

Greiser JS, Stross C, Heinrich PC, Behrmann I, Hermanns HM. Orientational constraints of the gp130 intracellular juxtamembrane domain for signaling. J Biol Chem 2002;277:26959–26965. [PubMed: 12011064]

Hage T, Sebald W, Reinemer P. Crystal structure of the interleukin-4/receptor alpha chain complex reveals a mosaic binding interface. Cell 1999;97:271–281. [PubMed: 10219247]

Hilton DJ, Zhang JG, Metcalf D, Alexander WS, Nicola NA, Willson TA. Cloning and characterization of a binding subunit of the interleukin 13 receptor that is also a component of the interleukin 4 receptor. Proc Natl Acad Sci U S A 1996;93:497–501. [PubMed: 8552669]

Kelly-Welch AE, Hanson EM, Boothby MR, Keegan AD. Interleukin-4 and interleukin-13 signaling connections maps. Science 2003;300:1527–1528. [PubMed: 12791978]

Kraich M, Klein M, Patino E, Harrer H, Nickel J, Sebald W, Mueller TD. A modular interface of IL-4 allows for scalable affinity without affecting specificity for the IL-4 receptor. BMC Biol 2006;4:13. [PubMed: 16640778]

Lai SY, Xu W, Gaffen SL, Liu KD, Longmore GD, Greene WC, Goldsmith MA. The molecular role of the common gamma c subunit in signal transduction reveals functional asymmetry within multimeric cytokine receptor complexes. Proc Natl Acad Sci U S A 1996;93:231–235. [PubMed: 8552611]

Laskowksi RA, MacArthur MW, Moss DS, Thornton JM. PROCHECK: a program to check the stereochemical quality of a protein structure. J Appl Crystallogr 1993;26:283.

Leonard, WJ. Type I Cytokines and Interferons and their Receptors. In: Paul, W., editor. Fundamental Immunology. Philadelphia: Lippinscott-Raven; 1999. p. 741-774.

Leonard WJ, Noguchi M, Russell SM. Sharing of a common gamma chain, gamma c, by the IL-2, IL-4, and IL-7 receptors: implications for X-linked severe combined immunodeficiency (XSCID). Adv Exp Med Biol 1994;365:225–232. [PubMed: 7887307]

Livnah O, Johnson DL, Stura EA, Farrell FX, Barbone FP, You Y, Liu KD, Goldsmith MA, He W, Krause CD, et al. An antagonist peptide-EPO receptor complex suggests that receptor dimerization is not sufficient for activation. Nat Struct Biol 1998;5:993–1004. [PubMed: 9808045]

McCoy AJ. Solving structures of protein complexes by molecular replacement with Phaser. Acta Crystallogr D Biol Crystallogr 2007;63:32–41. [PubMed: 17164524]

Miloux B, Laurent P, Bonnin O, Lupker J, Caput D, Vita N, Ferrara P. Cloning of the human IL-13R alpha1 chain and reconstitution with the IL4R alpha of a functional IL-4/IL-13 receptor complex. FEBS Lett 1997;401:163–166. [PubMed: 9013879]

Moy FJ, Diblasio E, Wilhelm J, Powers R. Solution structure of human IL-13 and implication for receptor binding. J Mol Biol 2001;310:219–230. [PubMed: 11419948]

Mueller TD, Zhang JL, Sebald W, Duschl A. Structure, binding, and antagonists in the IL-4/IL-13 receptor system. Biochim Biophys Acta 2002;1592:237–250. [PubMed: 12421669]

Murata T, Taguchi J, Puri RK. Interleukin-13 receptor alpha' but not alpha chain: a functional component of interleukin-4 receptors. Blood 1998;91:3884–3891. [PubMed: 9573026]

Murshudov GN, Vagin AA, Dodson EJ. Refinement of macromolecular structures by the maximum-likelihood method. Acta Crystallogr D Biol Crystallogr 1997;53:240–255. [PubMed: 15299926]

Nelms K, Keegan AD, Zamorano J, Ryan JJ, Paul WE. The IL-4 receptor: signaling mechanisms and biologic functions. Annu Rev Immunol 1999;17:701–738. [PubMed: 10358772]

Noguchi M, Yi H, Rosenblatt HM, Filipovich AH, Adelstein S, Modi WS, McBride OW, Leonard WJ. Interleukin-2 receptor gamma chain mutation results in X-linked severe combined immunodeficiency in humans. Cell 1993;73:147–157. [PubMed: 8462096]

Obiri NI, Debinski W, Leonard WJ, Puri RK. Receptor for interleukin 13. Interaction with interleukin 4 by a mechanism that does not involve the common gamma chain shared by receptors for interleukins 2, 4, 7, 9, and 15. J Biol Chem 1995;270:8797–8804. [PubMed: 7721786]

Otwinowski Z, Minor W. Processing of X-ray diffraction data collected in oscillation mode. Methods Enzymol 1997;276:307–326.

Ozaki K, Leonard WJ. Cytokine and cytokine receptor pleiotropy and redundancy. J Biol Chem 2002;277:29355–29358. [PubMed: 12072446]

Pandey A, Ozaki K, Baumann H, Levin SD, Puel A, Farr AG, Ziegler SF, Leonard WJ, Lodish HF. Cloning of a receptor subunit required for signaling by thymic stromal lymphopoietin. Nat Immunol 2000;1:59–64. [PubMed: 10881176]

Park LS, Friend D, Sassenfeld HM, Urdal DL. Characterization of the human B cell stimulatory factor 1 receptor. J Exp Med 1987;166:476–488. [PubMed: 3496417]

Rickert M, Wang X, Boulanger MJ, Goriatcheva N, Garcia KC. The structure of interleukin-2 complexed with its alpha receptor. Science 2005;308:1477–1480. [PubMed: 15933202]

Russell SM, Keegan AD, Harada N, Nakamura Y, Noguchi M, Leland P, Friedmann MC, Miyajima A, Puri RK, Paul WE, et al. Interleukin-2 receptor gamma chain: a functional component of the interleukin-4 receptor. Science 1993;262:1880–1883. [PubMed: 8266078]

Seder RA, Paul WE. Acquisition of lymphokine-producing phenotype by CD4+ T cells. Annu Rev Immunol 1994;12:635–673. [PubMed: 7912089]

Socolovsky M, Fallon AE, Lodish HF. The prolactin receptor rescues EpoR−/− erythroid progenitors and replaces EpoR in a synergistic interaction with c-kit. Blood 1998;92:1491–1496. [PubMed: 9716574]

Stroud RM, Wells JA. Mechanistic diversity of cytokine receptor signaling across cell membranes. Sci STKE 2004;2004:re7. [PubMed: 15126678]

Vagin A, Teplyakov A. An approach to multi-copy search in molecular replacement. Acta Crystallogr D Biol Crystallogr 2000;56:1622–1624. [PubMed: 11092928]

Waldmann TA. The biology of interleukin-2 and interleukin-15: implications for cancer therapy and vaccine design. Nat Rev Immunol 2006;6:595–601. [PubMed: 16868550]

Walter MR, Cook WJ, Zhao BG, Cameron RP Jr, Ealick SE, Walter RL Jr, Reichert P, Nagabhushan TL, Trotta PP, Bugg CE. Crystal structure of recombinant human interleukin-4. J Biol Chem 1992;267:20371–20376. [PubMed: 1400355]

Wang X, Rickert M, Garcia KC. Structure of the quaternary complex of interleukin-2 with its alpha, beta, and gammac receptors. Science 2005;310:1159–1163. [PubMed: 16293754]

Wills-Karp M. Interleukin-13 in asthma pathogenesis. Curr Allergy Asthma Rep 2004;4:123–131. [PubMed: 14769261]

Wlodawer A, Pavlovsky A, Gustchina A. Crystal structure of human recombinant interleukin-4 at 2.25 A resolution. FEBS Lett 1992;309:59–64. [PubMed: 1511746]

Zamorano J, Wang HY, Wang LM, Pierce JH, Keegan AD. IL-4 protects cells from apoptosis via the insulin receptor substrate pathway and a second independent signaling pathway. J Immunol 1996;157:4926–4934. [PubMed: 8943397]

Zhang JL, Buehner M, Sebald W. Functional epitope of common gamma chain for interleukin-4 binding. Eur J Biochem 2002;269:1490–1499. [PubMed: 11874464]

Zhang JL, Simeonowa I, Wang Y, Sebald W. The high-affinity interaction of human IL-4 and the receptor alpha chain is constituted by two independent binding clusters. J Mol Biol 2002;315:399–407. [PubMed: 11786020]

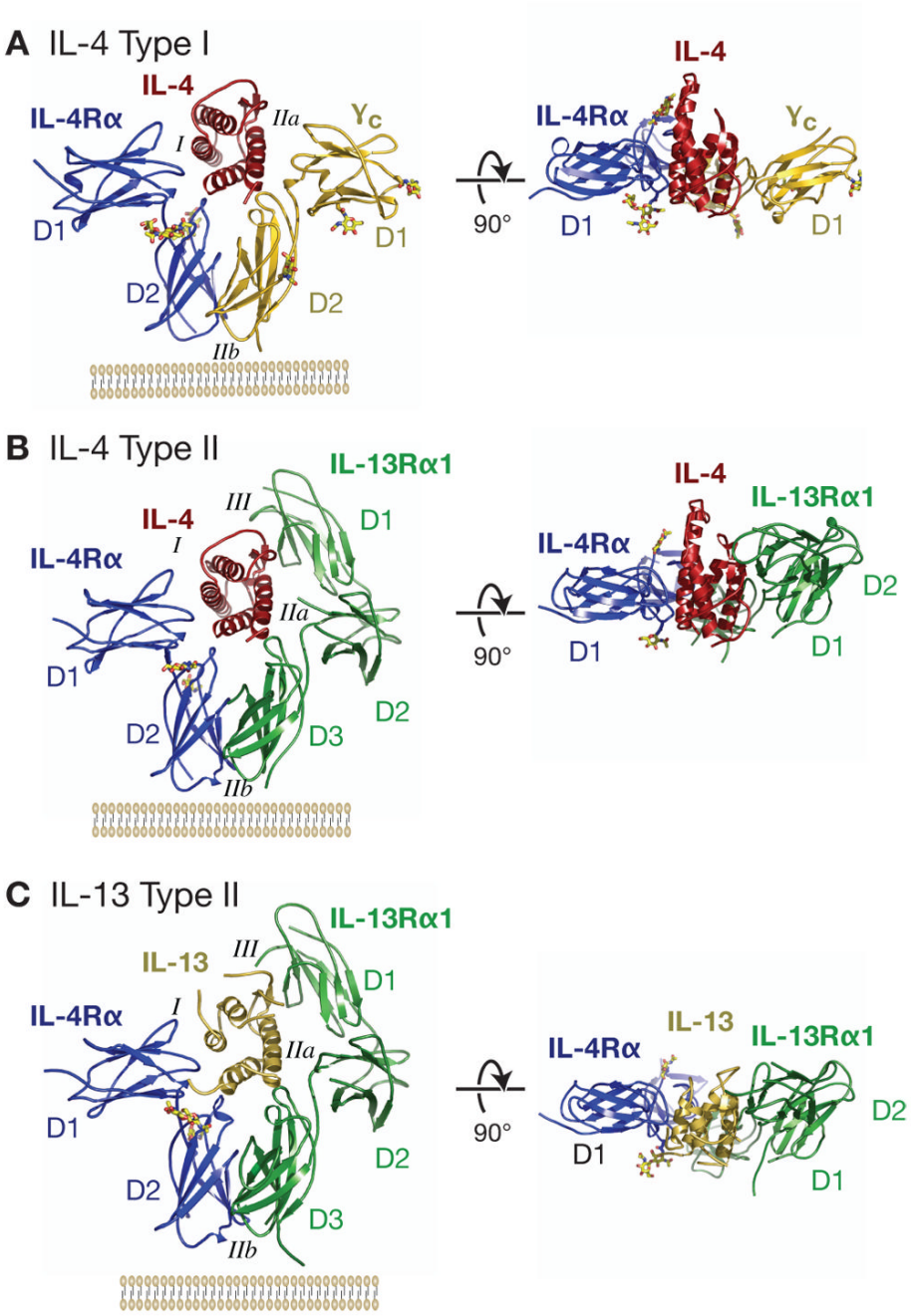

Figure 1. Structures of the Type I IL-4, Type II IL-4, and Type II IL-13 ternary complexes

(**A**) The Type I complex between IL-4Rα (blue), IL-4 (red) and γ_c (gold). (**B**) The Type II IL-4 complex between IL-4Rα (blue), IL-4 (red) and IL-13Rα1 (green). (**C**) The Type II IL-13 complex with IL-4Rα (blue), IL-13 (yellow-orange) and IL-13Rα1 (green). The complexes are shown from the side with a cartoon of a membrane underneath (left), and as viewed from the "top" (right). Glycan moieties on Asn residues are shown in ball-and-stick representation. All figures were generated with PyMol (DeLano, The PyMOL Molecular Graphics System, 2002).

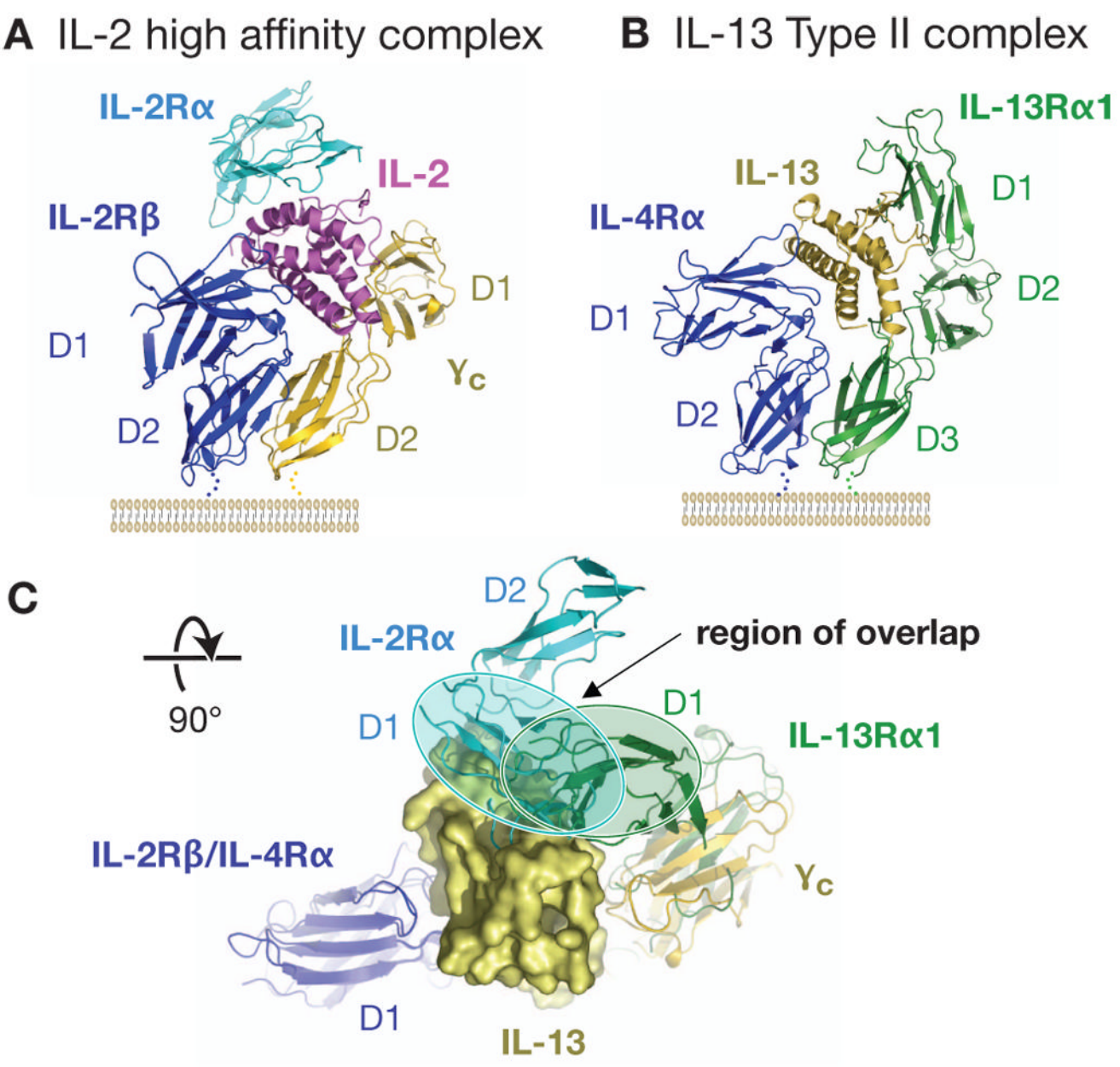

Figure 2. Structural similarity between IL-2Rα and IL-13Rα1 cytokine engagement

(**A**) The quaternary complex of IL-2 (pink), IL-2Rα (cyan), IL-2Rβ (blue) and γ_c (gold). IL-2Rα is bound to the top surface of IL-2. (**B**) Ternary complex of IL-13 (yellow-orange), IL-4Rα (blue), and IL-13Rα1 (green). (**C**) As viewed from the top, the overlapping cytokine binding sites by IL-2Rα and IL-13Rα1 D1 domains are apparent. Semi-transparent ovals have been drawn around the D1 domain of IL-2Rα and IL-13Rα1 so that regions of overlap are clear.

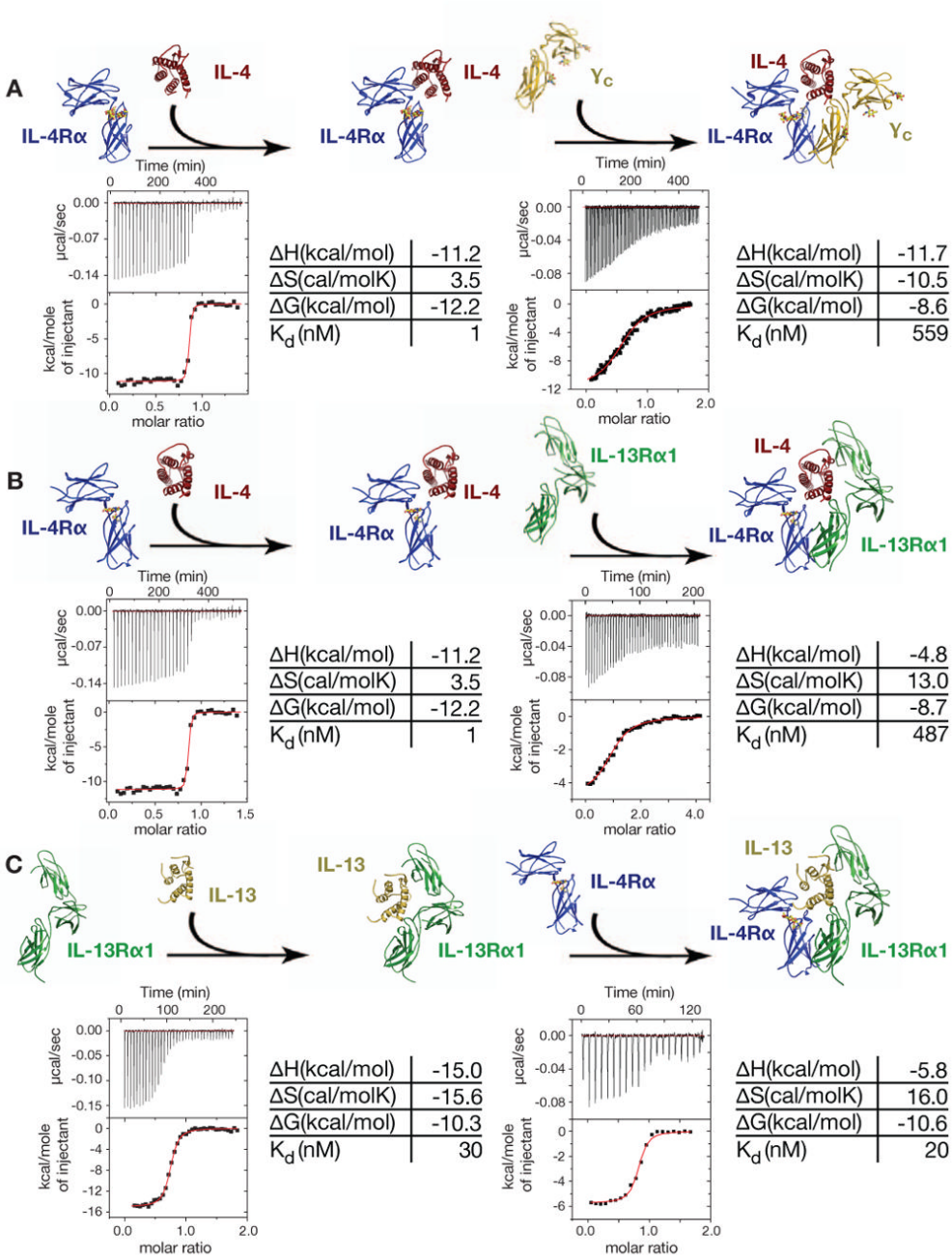

Figure 3. Contrasting assembly sequences, binding thermodynamics and stabilities of the three ternary complexes

Each row illustrates the reaction in the order in which the binary and ternary complexes assemble (color scheme is maintained from Figure 1). Inset tables list the thermodynamic parameters calculated based upon the isothermal titration calorimetry (ITC) binding isotherm shown below each reaction diagram. Data are also summarized in Table S3 (**A**) Type I complex: Reaction diagram for the interaction of IL-4Rα and IL-4 followed by recruitment of the second receptor, γ_c. (**B**) Type II IL-4 complex: the interaction of IL-4Rα and IL-4 followed by the recruitment of the second receptor, IL-13Rα1. In both (**A**) and (**B**), the extremely high affinity of IL-4/IL-4Rα (K_d < 1nM) is an estimate due to the steepness of the ITC trace. (**C**) Type II

IL-13 complex: the interaction of IL-13Rα1 and IL-13 followed by the recruitment of the second receptor, IL-4Rα.

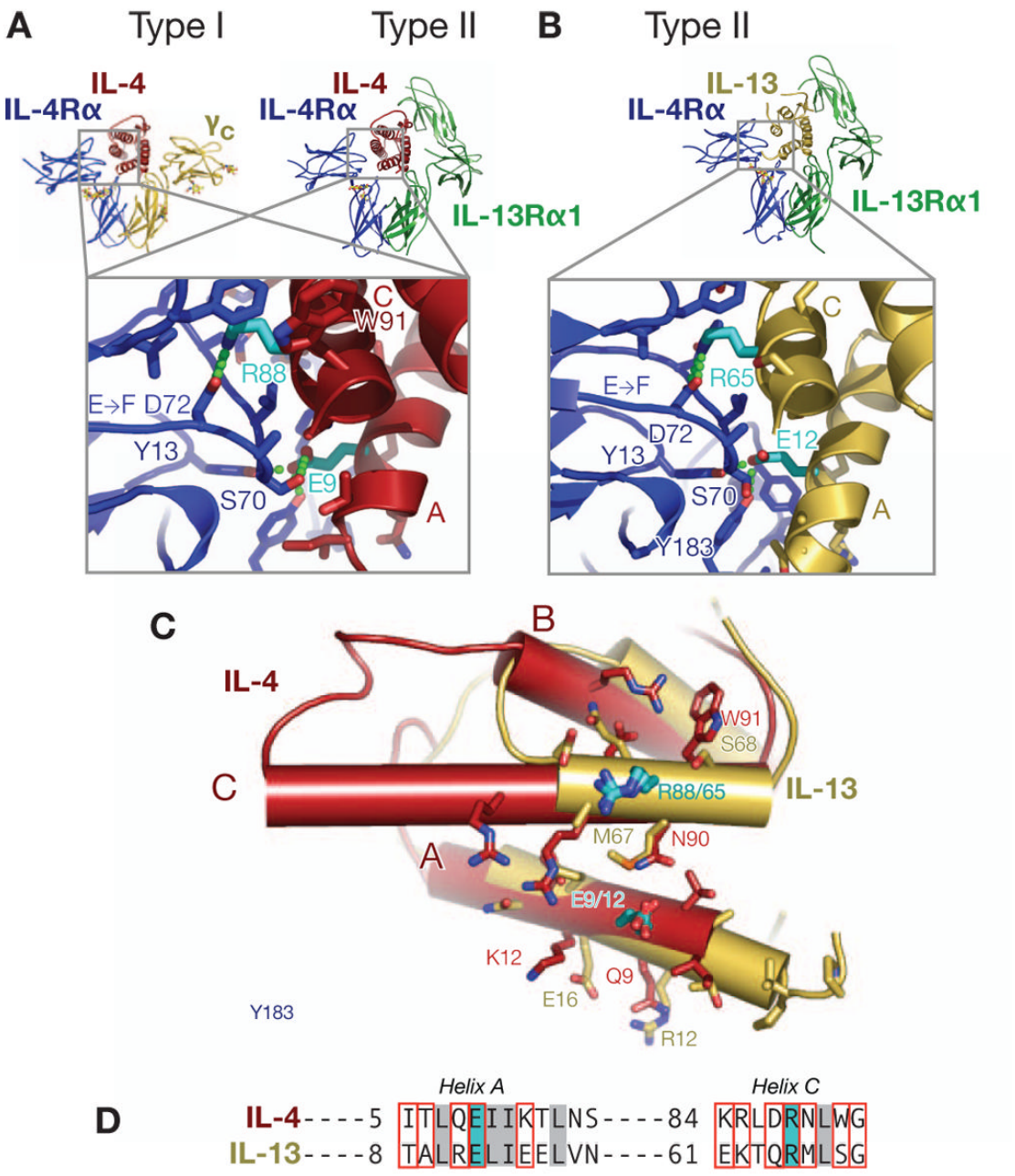

Figure 4. The interactions of IL-4Rα with IL-4 and IL-13

For clarity the overall complexes are shown above blowups of the site I IL-4 (**A**) and IL-13 (**B**) interfaces, with color scheme retained from Figure 1. Zoomed up region of the site I interfaces focuses on the IL-4Rα EF loop interactions with cytokine A and C helices (labeled). Key interacting residues are shown in stick representation, and the "mimicked" Arg and Glu hotspot residues found in both IL-4 and IL-13 are thicker sticks and colored cyan, with polar contacts drawn as dashed green lines. (**C**) "Open book" view of binding epitopes presented by IL-4 and IL-13 to IL-4Rα. The resulting IL-4 and IL-13 cytokine (shown as cylinders) positions after their respective IL-4Rα were superimposed shows the relative structural overlap of the cytokine site I binding sites. (**D**) Structure-based sequence alignment between the interacting

portions of helices A and C of IL-4 and IL-13 with IL-4Rα, where contact positions are in red boxes, common hydrophobic core residues are highlighted in gray and “hot spot” residues are highlighted in cyan to coincide with panels (A), (B) and (C).

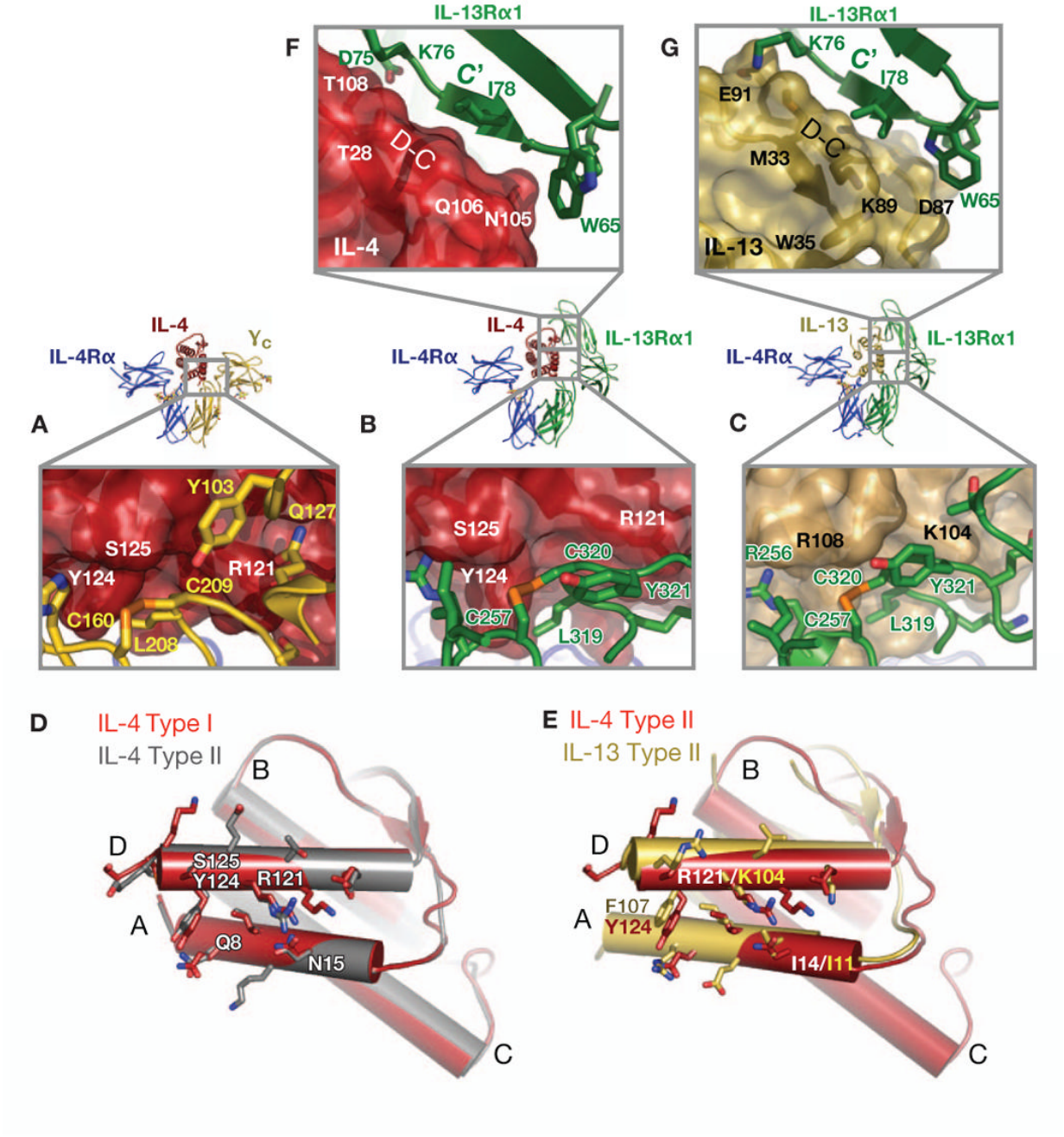

Figure 5. The interactions of IL-4 and IL-13 with γ_c and IL-13Rα1

For clarity the overall complexes are shown in between blowups of the site IIa (underneath) and III (above) interfaces using the same color scheme as previous figures. Panels (**A**), (**B**) and (**C**) show zoomed views of the site IIa interfaces of the IL-4 Type I, IL-4 Type II, and IL-13 Type II complexes, respectively, where the receptor residues are projected on semi-transparent cytokine surfaces. IL-4(red) and IL-13(yellow-orange) residues underneath the surfaces are labeled in white and black, respectively, while γ_c (gold) and IL-13 Rα1(green) residues are labeled in yellow and green, respectively. (**D**) and (**E**) "Open book" views of the site IIa binding sites. Panel (**D**) shows the resulting structural positions of IL-4 on IL-4 after superposition of IL-4Rα from the Type I and Type II complexes, and panel (**E**) shows the resulting structural

positions of IL-4 on IL-13 after superposition of IL-4Rα from the two different Type II complexes. All interacting residues in the site IIa interfaces are shown as sticks. Panels (**F**) and (**G**) illustrate the site III interfaces in IL-4 and IL-13 Type II complexes, respectively, using a similar coloring and labeling scheme as above. The anti-parallel beta sheet between the IL-13Rα1 c' strand the cytokine C–D loop is labeled.

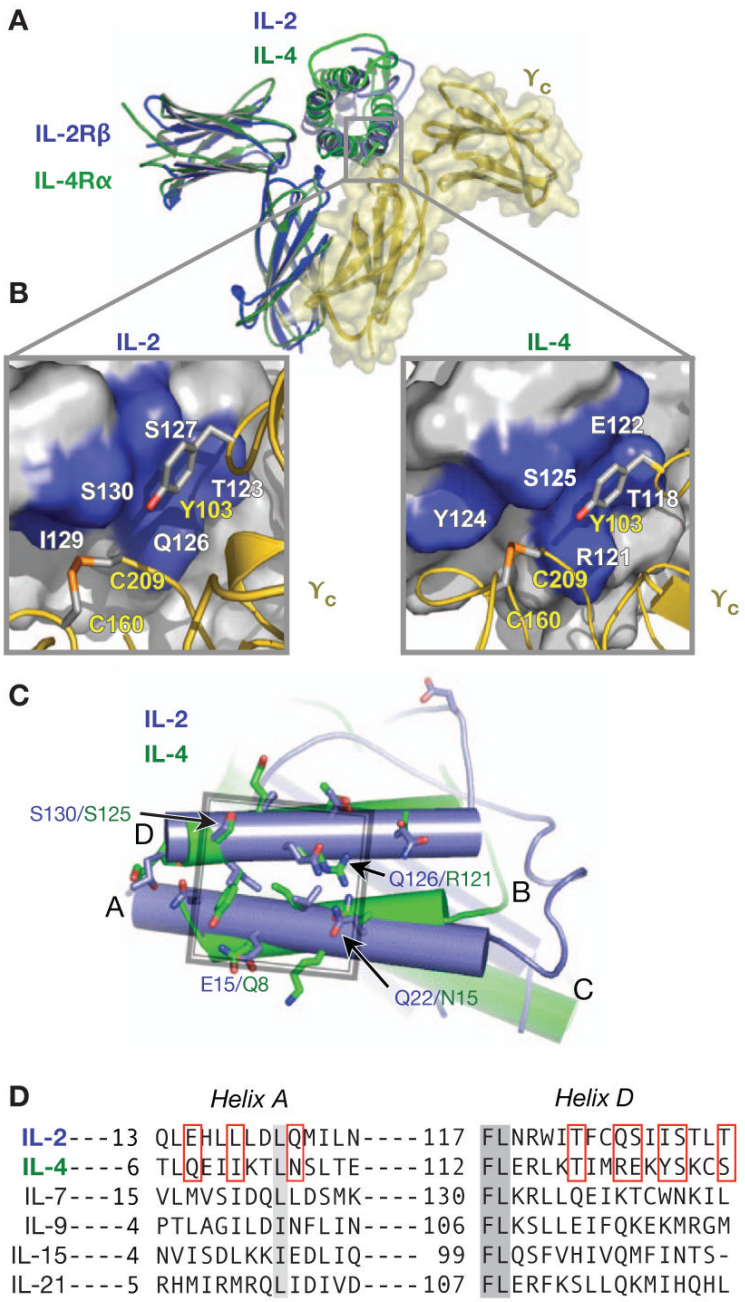

Figure 6. Basis of cross-reactive cytokine recognition by γ_c

(**A**) Structural alignment of the IL-2 quaternary (IL-2Rα not shown), and IL-4 Type I ternary complexes after superposition on γ_c (gold). The IL-2 complex is blue, and the IL-4 complex is green. (**B**) The conserved apolar 'canyon' on the cytokine surfaces (highlighted in blue) accommodates the protruding γ_c binding loops (gold and silver residues). (**C**) "Open book" views of the overlap of IL-2 versus IL-4 site IIa binding sites after superposition of γ_c. (**D**) Structure-based sequence alignment of all known γ_c cytokines for helices A and D based on γ_c contact positions by IL-2 and IL-4. Residue numbers are included and contact residues from IL-2 and IL-4 are marked with red boxes. Hydrophobic residues are shaded in gray and correspond predominantly with buried core residues.

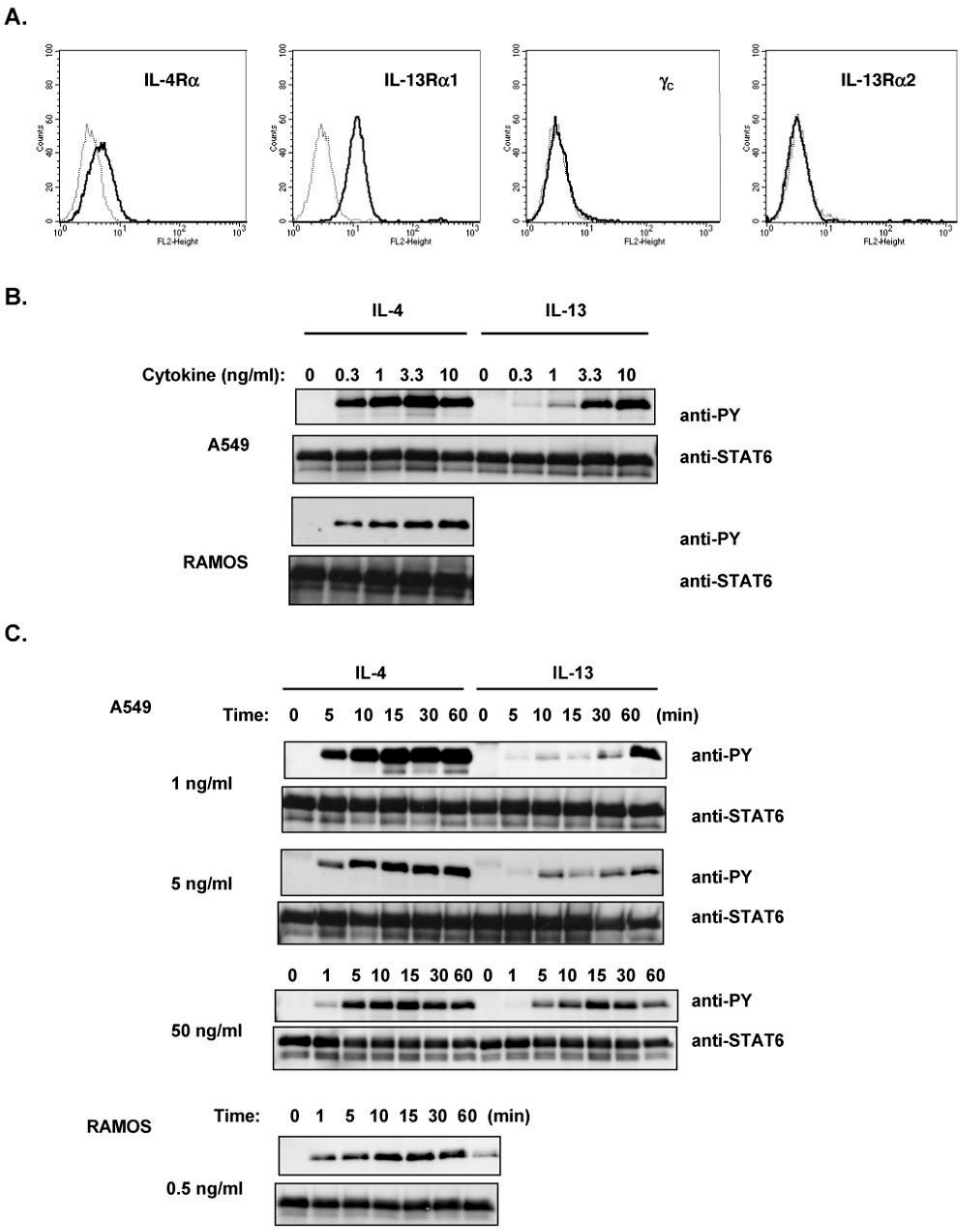

Figure 7. Comparison of signaling activated by IL-4 and IL-13

(**A**) A549 express IL-4Rα and IL-13Rα1, but not IL-13Rα2 or γ_c. Expression of receptor subunits on A549 was analyzed by FACS as described in Methods. The heavy black histograms indicate staining with specific antibody and the dotted histograms indicate staining by the isotype-matched control. (**B**) A549 cells and Ramos cells were washed and treated with various concentrations of IL-4 or IL-13 as indicated for 30 minutes. Cell lysates were prepared and immunoprecipitated with anti-STAT6. Western blots were probed with anti-phosphotyrosine antibody. The blots were stripped and reprobed with anti-STAT6. STAT3 activation is analyzed in Figure S6. (**C**) A549 cells and Ramos cells were treated with various concentrations

of IL-4 or IL-13 for various times; STAT6 phosphorylation was analyzed as described in (**B**). Data is quantitated in graphical format in Figure S7.